scientific reports

OPEN

Enhanced removal of organic dyes from aqueous solutions by new magnetic HKUST-1: facile strategy for synthesis

Masoumeh Mohammadnejad[1]✉, Niosha Mokhtari Nekoo[1], Sedighe Alizadeh[1], Soosan Sadeghi[1] & Shokoofeh Geranmayeh[2]

A novel, magnetic HKUST-1 MOF based on $MgFe_2O_4$-NH_2 was designed and synthesized in two steps and applied effective removal of malachite green (MG), crystal violet (CV), and methylene blue (MB) from water samples. Characterization of the newly synthesized $MgFe_2O_4$-NH_2-HKUST-1 was performed by various techniques such as Fourier transform infrared spectroscopy, X-ray diffraction, Field emission scanning electron microscopy, Brunauer–Emmett–Teller, Thermal gravimetric analysis, and Vibration sampling magnetometry. Malachite green, crystal violet and methylene blue are toxic and mutagenic dyes that can be released into the water in different ways and cause many problems for human health and the environment. The removal of malachite green, crystal violet, and methylene blue from aqueous solutions was investigated using the magnetic HKUST-1 in this research. The effect of various parameters such as pH, amount of sorbent, dye concentration, temperature, and contact time on dye removal has been studied. The results showed that more than 75% of dyes were removed within 5 min. Adsorption isotherms, Kinetic, and thermodynamic studies were investigated. The results of this study show that adsorption capacity of the magnetic adsorbent is equal to 108.69 mg g^{-1} for MG, 70.42 mg g^{-1} for CV, and 156.25 mg g^{-1} for MB. This study shows the good strategy for the synthesis of the functionalized magnetic form of HKUST-1 and its capability for increasing the efficiency of the removal process of malachite green, crystal violet, and methylene blue from an aqueous solution.

Water is the source of life on Earth. The life and health of humans and other living depend on this valuable substance. Environmental problems and the release of organic dyes into water sources are important concerns in the world. Water pollution is one of the most serious and important problems in the world, which cause many problems in human society. Therefore, effective and efficient removal of pollutants from water is very important[1]. One of the main factors of environmental pollution is the growth of chemical industries. Many chemical industries such as paper, plastic, cosmetics, leather, printing, pharmaceutical, and textile use synthetic dyes to color their products. These dyes release into the water and cause the production of wastewater with dyes and organic contents. Malachite green, Crystal violet, and methylene blue are cationic triphenylmethane dyes that are used for different purposes in the industry[2,3]. Malachite green is an organic compound that is widely used in aquaculture to treat fungal attacks and protozoal infections and is used in other industries such as food, health, and textile industries[4,5]. However, the use of this dye has raised many concerns due to its reported toxic effects. Although the use of this dye is prohibited in several countries and is not approved by the United States Food and Drug Administration, it is still used in many parts of the world due to its low cost, availability, and efficiency[5,6]. Crystal violet is widely used in veterinary medicine as a biological stain, it is also used as a textile dye in textile processing[3]. Also, methylene blue is the most common material used to dye cotton, wool, and silk. It can cause eye burns that may cause permanent eye damage. In case of inhalation, it can lead to acute respiratory problems, while oral consumption causes a burning sensation and may cause nausea, vomiting, profuse sweating, and mental confusion[7,8]. These dyes are toxic, carcinogenic, mutagenic, and often stable against light and heat[9]. As access to clean water is essential for various activities, removing these dyes from water and wastewater

[1]Department of Analytical Chemistry, Faculty of Chemistry, Alzahra University, Tehran, Iran. [2]Department of Physical Chemistry and Nanochemistry, Faculty of Chemistry, Alzahra University, Tehran, Iran. ✉email: m.mohammadnejad@alzahra.ac.ir; masoumeh.mohammadnejad@gmail.com

1

requires an efficient sorbent. In the present study, the efficient removal of malachite green, crystal violet, and methylene blue was done using an efficient synthetic sorbent based on magnetic MOF. The dyes studied in this research are presented in Table 1.

Metal-organic frameworks (MOFs) are porous structures that are created from the coordinated bond between metal ions and organic linkers or bridging ligands[10]. The specific structural characteristics of MOFs include a wide range of particle sizes, high surface-to-volume ratio, high absorption tendency, controllability of particle size, and high absorption capacity[11]. Due to their high surface area, tunable structural properties, and thermal stability, MOFs are suitable for a wide range of applications, including catalysis[12], gas storage[13], enzyme carriers[14], sensors[15], and as a sorbent in the adsorption process has been studied[4]. The absorption capacity of MOFs to adsorb dyes is significant. One of the significant advantages of MOF compared to other sorbents is its structural diversity, the possibility of determining the size of the pores, and their properties by choosing different metal Ions and organic ligands in the synthesis stages[16]. HKUST-1 MOF contains Cu^{2+} units coordinated by four carboxylate groups and creates a highly porous cubic structure with a 3D network[17,18]. The important point in manufacturing HKUST-1 is the easy and reproducible synthesis of this MOF. MOFs can be used to treat dyes wastewater. MOFs are suitable materials for dye adsorption from wastewater with favorable performance compared to conventional sorbents[19]. Recently, for the better performance of MOFs, their composites are used, and in this study, a magnetic composite has been synthesized. Among the sorbents that have been synthesized so far for the removal of pollutants, magnetic sorbents have received much attention for absorbing dyes[20].

Magnetic nanoparticles have attracted the attention of many researchers due to their extraordinary properties. They can be bound to MOFs by functionalization for the formation of a composite that has magnetic properties. Composites are a combination of two or more separate materials that have different properties than individual parts[21].

HKUST-1 has attracted the attention of researchers in recent years due to its easy and cost-effective synthesis. On the other hand, it is difficult to separate MOFs from the mixed solution and it causes secondary pollution in the environment, and a centrifugal step is needed to separate them from the aqueous solution, so the use of MOF magnetic adsorbent allows easy separation with an external magnetic field and product recovery It will be easy and the operating cost will be more affordable. Also, the stabilization of adsorbent in aqueous environments using composite formation, a short time in the removal process, and acceptable adsorbent capacity are important in this study. Therefore, the magnetic HKUST-1 has been considered an accepted and efficient adsorbent for its easy separation.

In this study, the synthesized $MgFe_2O_4$ nanoparticles were functionalized by the $-NH_2$ functional group to bind to the carboxylic acid group of HKUST-1 by hydrogen bonding. The new magnetic absorbent with the structure of $MgFe_2O_4$-NH_2-HKUST-1 was studied to remove dye pollutants methylene blue, crystal violet, and malachite green. This compound shows adequate adsorption capacity, speed, and removal percentage for removing dyes from wastewater. The effective factors, isotherms, kinetics, and thermodynamics of the adsorption removal process were investigated.

Experimental
Materials and instruments
Malachite green (MG), Crystal violet (CV), Methylene blue (MB), Iron (III) nitrate nonahydrate $Fe(NO_3)_3 \cdot 9H_2O$, Magnesium nitrate hexahydrate $Mg(NO_3)_2 \cdot 6H_2O$, Copper(II) nitrate trihydrate $Cu(NO_3)_2 \cdot 3H_2O$, benzene-1, 3,5-tricarboxylate (BTC), Sodium acetate $C_2H_3NaO_2$, Ethylene glycol $C_2H_6O_2$, Ethanolamine C_2H_7NO, Ethanol C_2H_5OH, Hydrochloric acid HCl were purchased from Merck and Sigma Aldrich company.

X-ray powder diffraction (XRD) measurements were performed using a Philips X'pert diffractometer with monochromatic Cu-Kα radiation. A glass pH electrode (Metrohm 713 pH-meter) was used for pH measurements. The morphology of samples was studied by field emission scanning electron microscopy (FE-SEM)

Dye	IUPAC name	Molecular formula	Molecular mass (g/mol)	Chemical structure
Malachite green oxalate	[4-[[4-(dimethylamino)phenyl]-phenylmethylidene]cyclohexa-2,5-dien-1-ylidene]-dimethylazanium;2-hydroxy-2-oxoacetate;oxalic acid	$C_{52}H_{54}N_4O_{12}$	927.0	
Crystal violet	[4[bis[4(dimethylamino)phenyl]methylidene]cyclohexa-2,5-dien-1-ylidene]-dimethylazanium;chloride	$C_{25}H_{30}ClN_3$	407.979	
Methylene blue	[7-(dimethylamino)phenothiazin-3-ylidene]-dimethylazanium;chloride	$C_{16}H_{18}ClN_3S$	319.85	

Table 1. Chemical characteristics of organic dyes studied in this research.

KYKY-EM 3200 with gold coating. Fourier transform infrared spectroscopy (FT-IR) spectra were obtained on Equinox 55 BRUKER model FT-IR spectrometer. The absorbance measurement was carried out by double-beam UV–Vis spectrophotometer using a 1 cm quartz cell (Perkin-Elmer, Lambda 35, USA). BET (Belsorp mini II, Microtrace bel Corop), TGA (Bahr, Germany), zeta potential (SZ-100z), and vibrating sample magnetometer (Lake Shore Cryotronics-7407) analysis were done.

Synthesis of MgFe$_2$O$_4$-NH$_2$

10 mmol of CH$_3$COONa as dissolved in 6.5 mL Ethylene glycol and heated to 100 °C under a magnetic stirring and refluxing system in the sand bath for 15 min. A solution of 0.66 mmol of Mg(NO$_3$)$_2$·6H$_2$O and 1.3 mmol of Fe(NO$_3$)$_3$·9H$_2$O dissolved in 3.5 mL ethylene glycol was poured into the preheated solution rapidly. The mixture was stirred for 30 min, and then 2.3 mL of ethanolamine was added. The mixture was heated to 200 °C and maintained for 12 h and then, the system was cooled to room temperature naturally. The black precipitate was collected by a magnetic separator, washed with double distilled water excessively, and then ethanol. The final product, the MgFe$_2$O$_4$-NH$_2$ nanoparticle, was dried at 70 °C for 4 h[22] (Scheme 1).

Synthesis of MgFe$_2$O$_4$-NH$_2$-HKUST-1 composite

0.05 g of the synthesized nanoparticle (MgFe$_2$O$_4$-NH$_2$) and 2.4 mmol of copper nitrate were dissolved in 25 ml of ethanol and placed in an ultrasonic bath for 30 min. Then 1 mmol of BTC was dissolved in 25 ml of ethanol and added to the previous solution at a rate of 0.5 mL/min under mechanical stirring for 1 h. Then, the final product (green precipitate) was washed several times with ethanol separated by an external magnet, and then dried under a temperature of 50 °C for 4 h in a vacuum oven (Scheme 2).

Adsorption process

Different solutions of dyes were prepared by dissolving appropriate amounts of MG, CV, and MB in the range of 0.18–9.27 mg L^{-1}, 0.81–6.94 mg L^{-1}, and 0.63–5.43 mg L^{-1}, respectively, in distilled water. The calibration curves were obtained by measuring the absorbance for MG at 620 nm, CV at 590 nm, and MB at 664 nm. The adsorption process was carried out by the addition of 10 mg, 5.5 mg, and, 1 mg of sorbent separately to the 5 mL solutions with different concentrations of MG, CV, and, MB (Scheme 3).
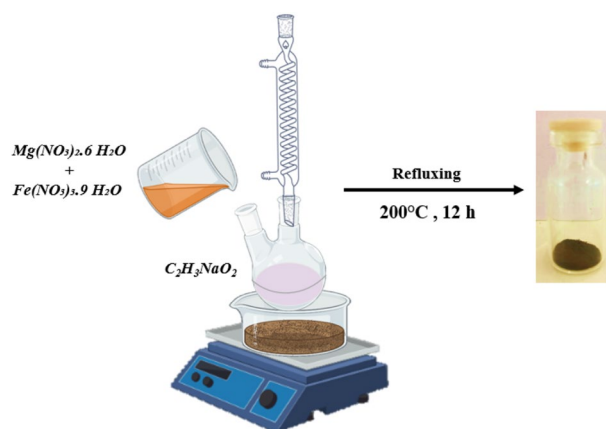
Scheme 1. The magnetic nanoparticle synthesis process.
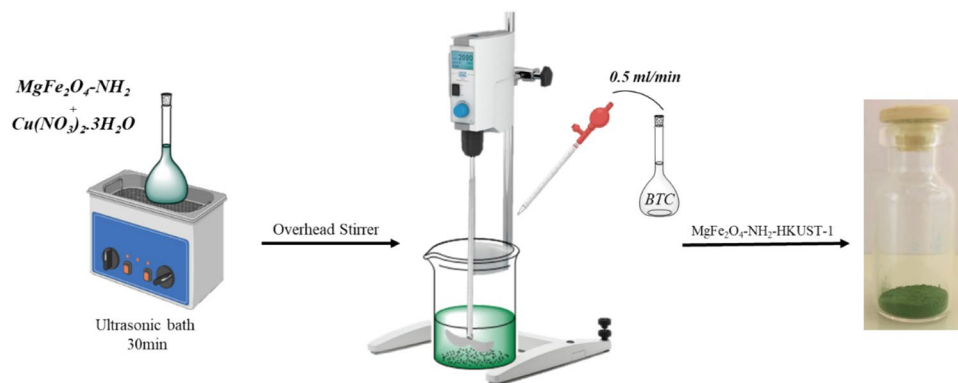
Scheme 2. The magnetic composite synthesis process.

3
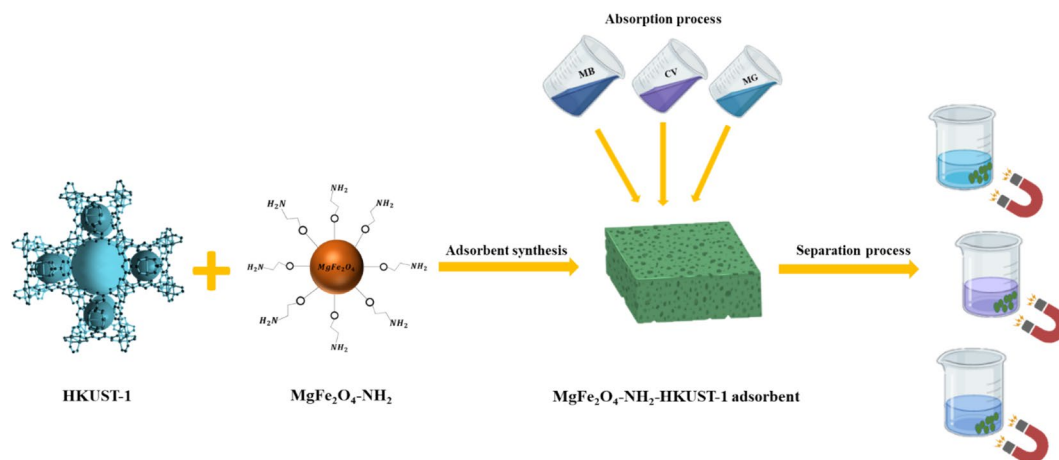
Scheme 3. The process of removing organic dyes and separating the sorbent from the solution.

The solutions including the sorbent were mixed with a magnetic stirrer for 5 min for all dyes. Subsequently, the sorbent was separated by an external magnet, and the remaining MG, CV, and MB concentrations were calculated by the following equation:

$$Removal\ (\%) = \left(1 - \frac{A}{A_0}\right) \times 100 \qquad (1)$$

where A is the adsorption of the analyte after adding the sorbent and A_0 is the initial adsorption of the solution.

Result and discussion
Characterization of MgFe$_2$O$_4$-NH$_2$-HKUST-1 composite
For characterization of prepared magnetic composite, FT-IR spectra (4000–400 cm^{-1}) in KBr pellet, X-ray powder diffraction (XRD) measurements, field emission scanning electron microscopy (FE-SEM), Brunauer–Emmett–Teller (BET), Thermal gravimetric analysis (TGA) and Vibrating sample magnetometer (VSM) were performed.

FT-IR analysis
The Fourier transform infrared (FT-IR) spectra of HKUST-1, MgFe$_2$O$_4$-NH$_2$, and MgFe$_2$O$_4$-NH$_2$-HKUST-1 have been shown in Fig. 1a.

In the FT-IR spectra related to HKUST-1 Bands in 1447 cm^{-1} and 1639 cm^{-1} are attributed to –O–C–O– groups, and the bands in 1375 cm^{-1} and 1565 cm^{-1} are attributed to the C=C stretching vibration of the BTC ligand. The band in 680 cm^{-1} is related to the Cu–O bond[23]. The broad peak at 3420 cm^{-1} can be attributed to the -OH of water molecules[24]. In the FT-IR spectra related to MgFe$_2$O$_4$-NH$_2$ the bands in 2923 cm^{-1} and 2856 cm^{-1} are attributed to the stretching vibration of the C–H bond in ethanolamine or ethylene glycol. The band in 1054 cm^{-1} can be attributed to the overlap of the C–O bond with the C–N stretching vibration, which is a sign of the binding of amine groups on the MgFe$_2$O$_4$-NH$_2$ nanoparticle[22], The band in 570 cm^{-1} is related to the Fe–O bond. Also, the bands in 1383 cm^{-1}, 1630 cm^{-1}, and 3420 cm^{-1} are related to C–N stretching vibration, NH$_2$ scissor bending vibration, and N–H stretching vibration, which indicates the presence of ethanolamine molecules on the nanoparticle surface[25].

Therefore, the peaks appearing in the spectrum of HKUST-1 and MgFe$_2$O$_4$-NH$_2$ can be seen in the spectrum corresponding to the synthesized composite.
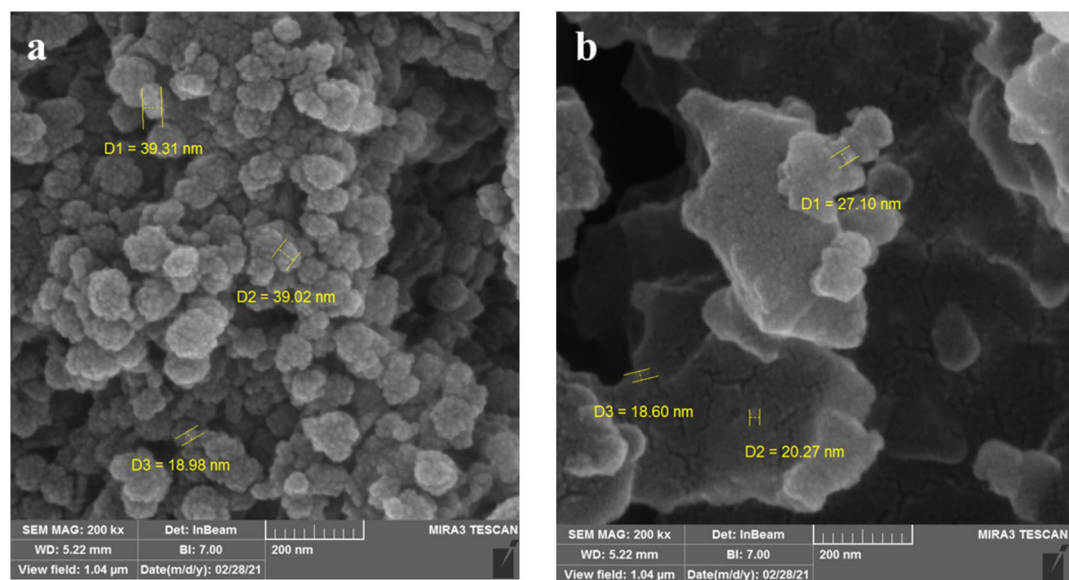
XRD analysis
To investigate the phase purity of the prepared sorbent, powder X-ray diffraction (XRD) was carried out (Fig. 1b). In the XRD pattern related to MgFe$_2$O$_4$-NH$_2$, peaks at the angles of $2\theta = 30.2°$, $35.44°$, $43.12°$, $56.8°$, and $62.48°$ are the characteristic peaks of the synthesized compound[25]. In the XRD pattern related to HKUST-1, the peaks in the angles of $2\theta = 11.5°$, $13.2°$, $16.3°$, $17.3°$, $20.0°$, $29.3°$, $35.40°$ are the characteristic peaks of this structure[23]. The peaks appearing in pattern of HKUST-1 and MgFe$_2$O$_4$-NH$_2$ can be seen in the pattern of the synthesized composite.

FE-SEM micrographs
FE-SEM was also carried out to observe the morphology of the MgFe$_2$O$_4$-NH$_2$-HKUST-1. In Fig. 2a, FE-SEM images of metal oxide nanoparticles MgFe$_2$O$_4$-NH$_2$ are given. These images show that the synthesized nanoparticles are spherical with an approximate diameter of 40 nm. In Fig. 2b, nanocomposite MgFe$_2$O$_4$-NH$_2$-HKUST-1 is given which can represent the synthesized magnetic composite framework.
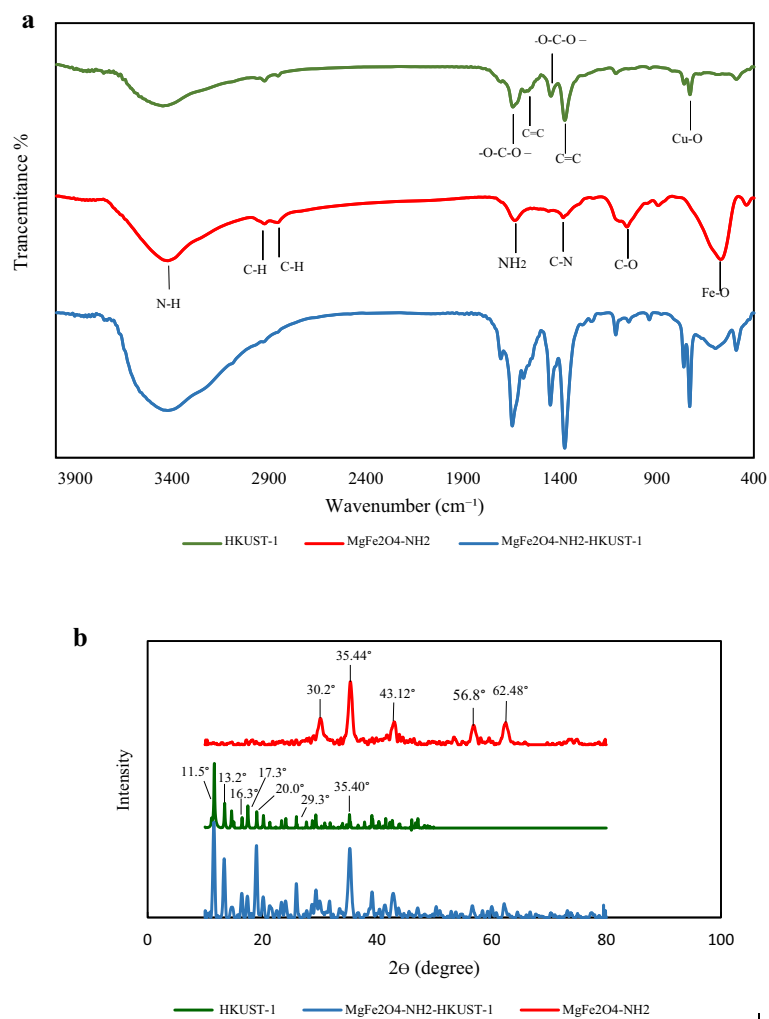
Figure 1. (**a**) FT-IR spectra of HKUST-1, $MgFe_2O_4$-NH_2 and $MgFe_2O_4$-NH_2-HKUST-1, (**b**) XRD pattern of $MgFe_2O_4$-NH_2, H KUST-1, and $MgFe_2O_4$-NH_2-HKUST-1.

Figure 2. (**a**) FE-SEM of $MgFe_2O_4$-NH_2, (**b**) FE-SEM of $MgFe_2O4$-NH_2-HKUST-1 magnetic composite.

BET analysis

The surface properties of the $MgFe_2O_4$-NH_2-HKUST-1, such as the surface area, and pore diameter were also examined using BET surface area analysis. The specific surface area of the $MgFe_2O_4$-NH_2-HKUST-1 composite evaluated was obtained at 297.13 m^2 g^{-1}. Also, average pore diameter distribution was investigated using the Barret–Joyner–Halenda (BJH) method. The average pore diameter of the synthesized composite was reported to be 4.26 nm (Table 2). The adsorption–desorption curve of nitrogen gas for the synthesized composite shows I/IV mixed type isotherm, which means $MgFe_2O_4$-NH_2 nanoparticles are with microporous and mesoporous structures at the same time, as shown in Fig. 3a.

TGA analysis

The thermal stability of the $MgFe_2O_4$-NH_2-HKUST-1 composite was estimated via TGA. The TGA profile depicted three weight loss steps in the tested temperature range of 50–700 °C (Fig. 3b). The first weight loss %20 appeared in the temperature range of 80–150 °C, which probably indicates the removal of surface water or residual solvent and physisorbed and chemisorbed H_2O molecules in the sample. In the second stage, in the temperature range of 150–420 °C, organic binders begin to degrade and eventually lead to the complete collapse of the composite, and the remaining mass in this stage reaches 45% of the initial mass. In the third stage, with an increase in temperature from 420 °C, an increase in mass of about 2% by weight is observed. This increase in mass can be due to the formation of some oxides that are not stable at higher temperatures and gradually decompose. Also, the approximate stability of the sample mass in the range of 40% of the initial mass can be attributed to the presence of CuO and Fe_3O_2 compounds[23,26–28].

Compound	Average pore diameter (nm)	Specific surface area (m^2 g^{-1})
$MgFe_2O_4$-NH_2-HKUST-1	4.26	297.13

Table 2. Information about the porosity of the synthesized composition.
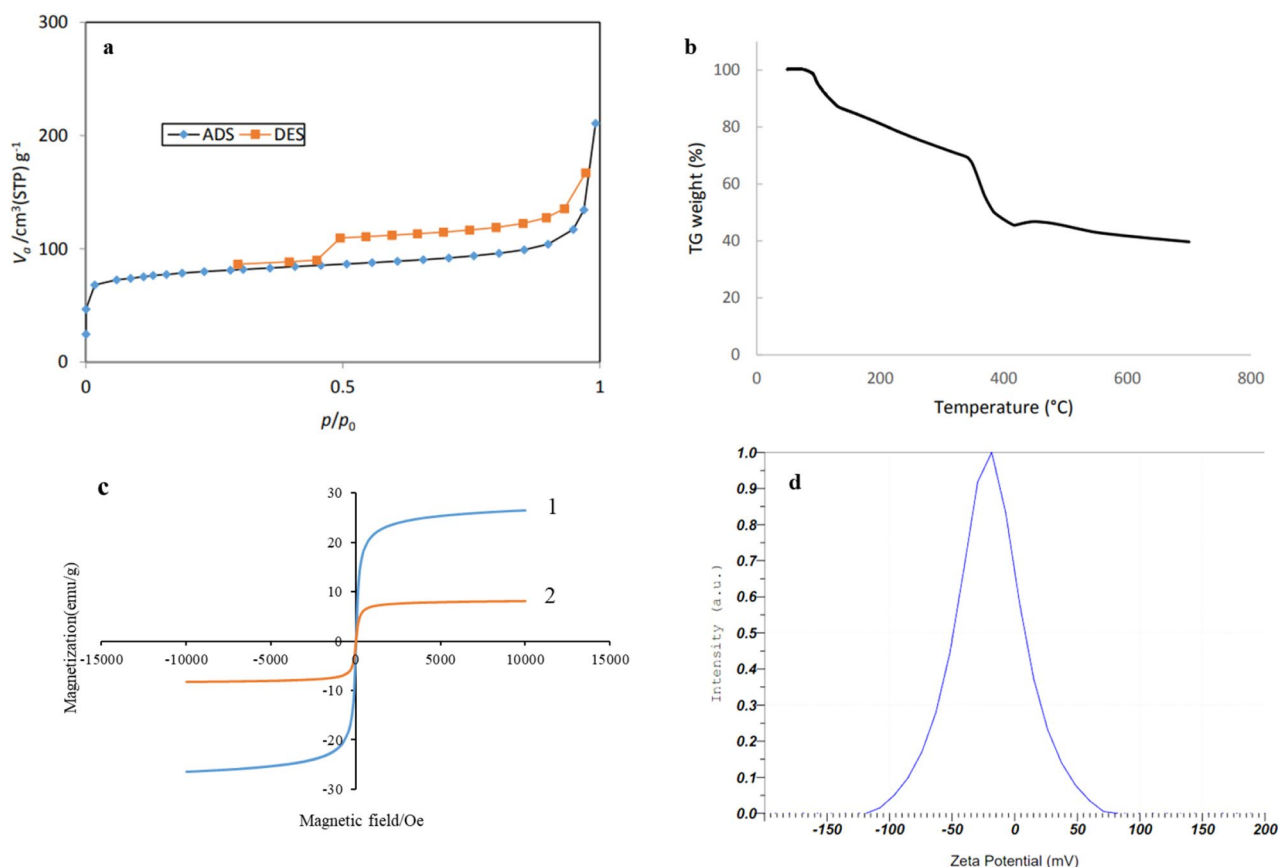
Figure 3. (**a**) Nitrogen gas adsorption–desorption curve for the synthesized composite. (**b**) The thermal analysis of $MgFe_2O_4$-NH_2-HKUST-1. (**c**) Magnetic analysis spectrum of (1) $MgFe_2O_4$-NH_2 magnetic nanoparticle, (2) $MgFe_2O_4$-NH_2-HKUST-1 magnetic composite. (**d**) Zeta potential of magnetic composite $MgFe_2O_4$-NH_2-HKUST-1.

VSM analysis

To study the magnetic behavior of MgFe$_2$O$_4$-NH$_2$ nanoparticles and MgFe$_2$O$_4$-NH$_2$-HKUST-1 composite, magnetization measurements were performed by VSM. As seen in (Fig. 3c (1), the value of saturation magnetic (Ms) was 28.48 emu g^{-1} for MgFe$_2$O$_4$-NH$_2$ nanoparticles and according to Fig. 3c (2), the maximum saturation magnetization of the MgFe$_2$O$_4$-NH$_2$-HKUST-1 composite was obtained 8.13 emu g^{-1}, which is enough to quickly collect it by a strong magnet. from a large volume of water. The amount of saturation magnetization of magnetic composite has decreased compared to magnetic nanoparticles, which can be caused by an increase in the thickness of the non-magnetic component. Also, due to the reduction of the coercivity force (H$_C$), it is concluded that the synthesized sorbent has superparamagnetic properties.

Zeta potential

To check the surface charge of the synthesized composite, the zeta potential was used. The zeta potential of the sorbent is one of the factors that can affect the adsorption capacity. According to Fig. 3d, the results showed that the surface charge of the synthesized sorbent is negative and equal to − 20.5 mV, so MG, CV, and MB cationic dyes are adsorbed on the surface of the sorbent.

## Optimization of experimental conditions for dyes removal

To obtain more effective adsorption of MG, CV, and MB, the effect of adsorption conditions was investigated and optimized. These parameters are initial solution pH, amount of sorbent, and contact time.

Initial solution pH

In this procedure, adsorption experiments of MG, CV, and, MB were done within the solution pH ranging from 3.0 to 10.0, and %removal was calculated (Fig. 4a–c). The adsorption capacities of MgFe$_2$O$_4$-NH$_2$-HKUST-1 for MG, CV, and MB increased with the solution pH increasing to 5.5, 5, and 7. However, the adsorption capacity decreased up to 10. According to the pK_a and cationic nature of these dyes at the mentioned pH and also based on the zeta potential analysis that shows the sorbent surface is negative it can be concluded these cationic dyes are protonated at the tested pH and are probably electrostatically adsorbed by the sorbent.

Amount of sorbent

The amount of sorbent could directly affect the adsorption capacity. To obtain the optimal adsorption conditions, experiments were carried out by the addition of 1–12.0 mg, 1–10 mg, and 0.25–5 mg of sorbents to a series of 5 mL of 1.3×10^{-5} mol/L solution of MG and CV and MB, respectively. The optimum weight of sorbent for the removal of MG, CV, and MB has obtained 10 mg, 5.5 mg, and 1 mg, respectively as shown in Fig. 4d–f.
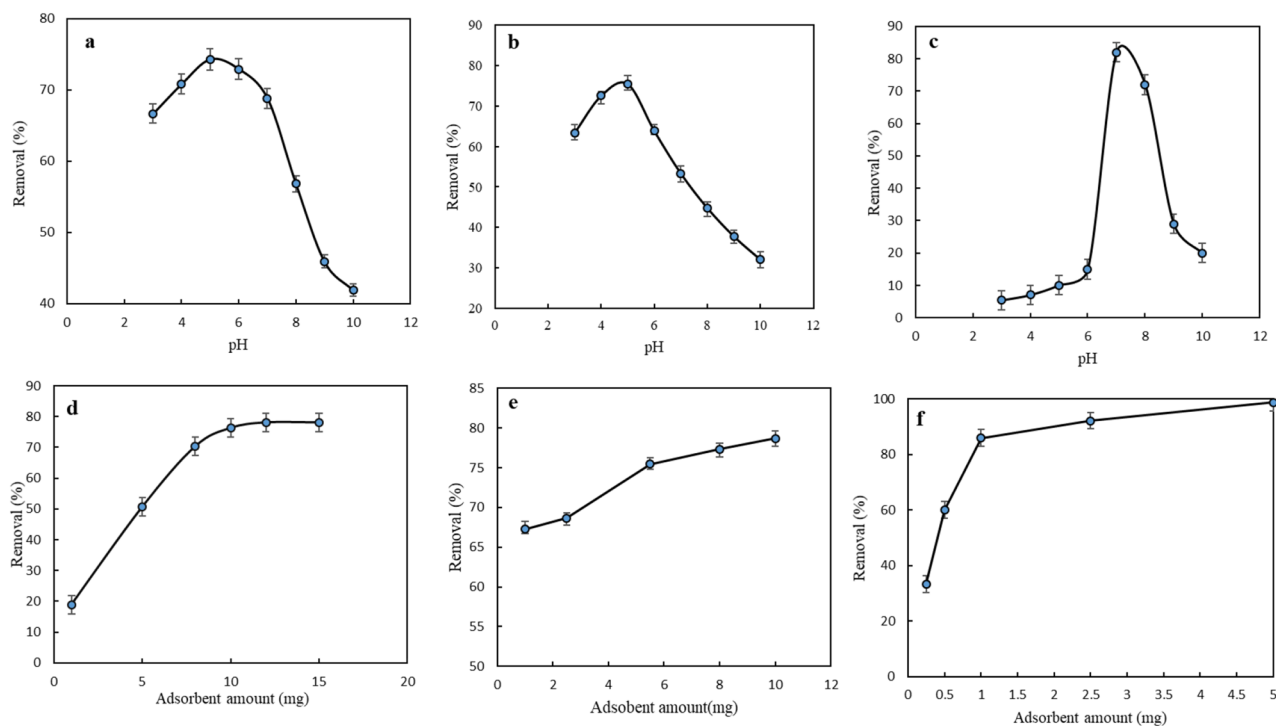
Figure 4. The effect of pH on the removal process of (**a**) MG, (**b**) CV, and (**c**) MB by the sorbent in the range of 3.0–10.0 and the graph of the removal percentage of (**d**) MG, (**e**) CV, and (**f**) MB from the solution according to the weight of the sorbent.

Adsorption time
The adsorption rate is an important factor. Absorbance spectra for MG, CV, and MB were recorded by time in the presence of sorbent. The optimal time for three dyes was 5 min, with a high removal percentage which is one of the excellent features of the synthesized sorbent.

Stability and reproducibility
According to the tests, the synthesized adsorbent can be used for at least 5 cycles without significant decrease in its efficiency. Also to check the reproducibility, adsorbents were synthesized in different times and removal experiments performed under the mentioned optimal conditions. The reproducibility of the adsorbent for 3 dyes is reported in Table 3.

Adsorption capacity and isotherm

To describe the adsorption mechanism for MG, CV, and MB, the values of $1/q_e$ versus $1/C_e$ were plotted for the Langmuir isotherm. The values of Ln q_e versus Ln C_e were plotted for the Freundlich isotherm. Equations (2) and (3) express the linear form of Langmuir and Freundlich isotherms, respectively:

$$\frac{1}{q_e} = \frac{1}{q_{max}K_LC_e} + \frac{1}{q_{max}} \tag{2}$$

$$Lnq_e = LnK_F + \frac{1}{n}LnC_e \tag{3}$$

where C_e (mg L^{-1}) represents the equilibrium concentration of MG, CV, and MB; q_e (mg g^{-1}) is the equilibrium adsorption capacity; q_{max} (mg g^{-1}) is the maximum adsorption capacity; K_L (L mg^{-1} or L mol^{-1}) is Langmuir constant represents the adsorption energy and K_F and n are the Freundlich constants[29]. Figure 5 and Table 4 show Langmuir and Freundlich isotherm diagrams and results for MG, CV, and MB.

Adsorption kinetics

Adsorption rate is an important characteristic for the evaluation of sorbents. Fast adsorption onto MgFe$_2$O$_4$-NH$_2$-HKUST-1 occurred in the initial adsorption stage. For example, more than 75% of dyes were removed within 5 min when the initial MG concentration was 10^{-5} mol/L with 10 mg of sorbent and CV concentration was 1.3×10^{-5} mol/L with 5.5 mg of sorbent, and MB concentration was 1.3×10^{-5} mol/L with 1 mg of sorbent. To further analyze and calculate the kinetic parameters, the experimental data were fitted by two kinetic models: the pseudo-first-order Eq. (4) and pseudo-second-order Eq. (5) kinetic models[30]:

$$Log(q_e - q_t) = Logq_e - \frac{k_1t}{2.303} \tag{4}$$
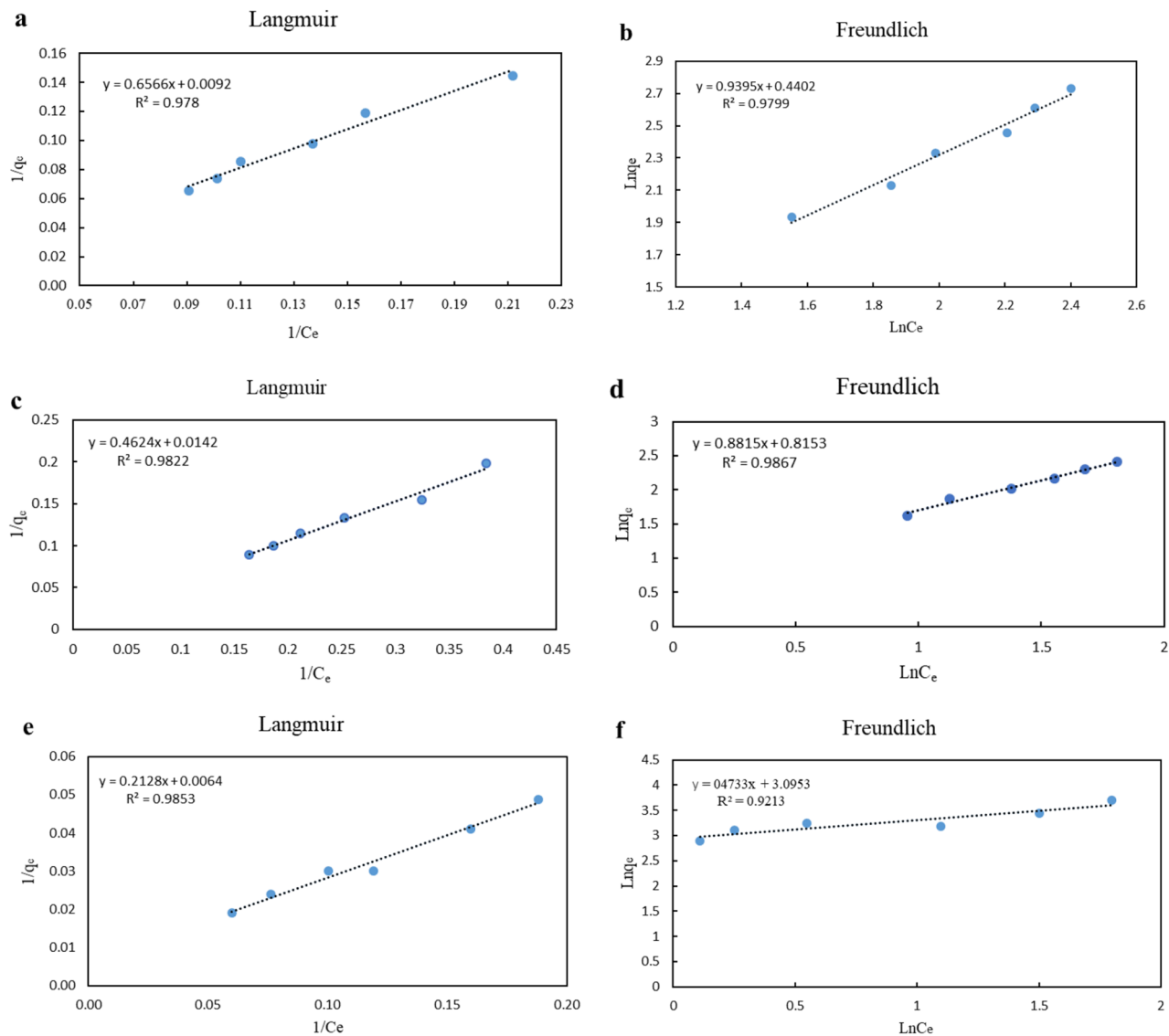
$$\frac{t}{q_t} = \frac{1}{k_2q_e^2} + \frac{t}{q_e} \tag{5}$$

where q_t (mg g^{-1}) and q_e (mg g^{-1}) are the amounts of MG, CV, and MB adsorbed at time t (min) and the amount at adsorption equilibrium, respectively, and k_1 (min^{-1}) and k_2 (g mg^{-1} min^{-1}) are the pseudo-first-order and pseudo-second-order rate constants, respectively.

The fitting results (Table 5) show that the adsorption of MG, CV, and MB onto MgFe$_2$O$_4$-NH$_2$-HKUST-1 could be well described by the pseudo-second-order kinetic model.

Test no	Analyte	pH	Amount of sorbent (mg)	Adsorption time (min)	% Removal	% RSD
1					75.6	
2	MG	5.5	10	5	74.7	0.88
3					75.8	
4					76.3	
1					76.6	
2	CV	5	5.5	5	75.8	0.75
3					75.3	
4					75.5	
1					82.8	
2	MB	7	1	5	84.9	1.04
3					83.5	
4					83.6	

Table 3. Reproducibility tests.

Figure 5. Langmuir and Freundlich isotherm diagram of MG (**a**,**b**), CV (**c**,**d**), and MB (**e**,**f**).

Constants	MG	CV	MB
Langmuir equation			
R^2	0.9780	0.9822	0.9853
q_{max} (mg g^{-1})	108.69	70.42	156.25
K_L (L mg^{-1})	0.01	0.03	0.03
R_L	0.91	0.85	0.97
Freundlich equation			
R^2	0.9799	0.9867	0.9213
K_F (mg g^{-1}) (L mg^{-1})$^{1/n}$	1.55	2.25	22.08
n	1.06	1.13	2.12

Table 4. Langmuir and Freundlich isotherm constants of MG, CV, and MB constants.

Adsorption thermodynamics

The thermodynamic parameters, standard free energy change ($\Delta G°$, kJ mol^{-1}), enthalpy change ($\Delta H°$, kJ mol^{-1}), and entropy change ($\Delta S°$, J mol^{-1} K^{-1}) related to the adsorption were determined. These parameters can be calculated with the following equations (Eqs. 6, 7).

Kinetic model	MG	CV	MB
Pseudo-first-order			
k_1 (min^{-1})	1.26	0.34	1.89
R^2	0.917	0.987	0.921
Pseudo-second-order			
k_2 (g mg^{-1} min^{-1})	4.94	3.68	0.765
R^2	0.996	0.999	0.993

Table 5. Pseudo-first-order and pseudo-second-order kinetic model.

$$\Delta G° = -RTLn\left(\frac{q_e}{C_e}\right) \tag{6}$$

$$\Delta G° = \Delta H° - T\Delta S° \tag{7}$$

where, T (K) is the temperature in Kelvin, R (8.314 J mol^{-1} K^{-1}) is the universal gas constant and K (L mol^{-1}) is the thermodynamic equilibrium constant for the adsorption process calculated from the ratio of the equilibrium adsorption capacity (q_e) to the equilibrium concentration of the solution (C_e).

The thermodynamic parameters were determined at 21,116 and 18,217 kJ mol^{-1} for ΔH and 75.493 and 67.856 J mol^{-1} K^{-1} for ΔS for MG and CV respectively. The results confirm an endothermic nature for MG and CV, as the temperature increases, the removal percentage of MG and CV increases. The adsorption process of these two dyes is a possible and spontaneous process. The thermodynamic parameters were determined − 7102.3 kJ mol^{-1} for ΔH and 6.05 mol^{-1} K^{-1} for ΔS for MB. Unlike MG and CV, the adsorption of MB decreased with increasing temperature and the adsorption process was exothermic.

The mechanism of the adsorption process

The organic dye adsorption process occurs because the adsorbent's surface particles are not in the same environment as the particles within the bulk. Inside the MgFe$_2$O$_4$-NH$_2$-HKUST-1, all of the forces acting between the particles are mutually balanced, but on the surface, the particles are not surrounded by atoms or molecules of their kind, and thus they have unbalanced or residual attractive forces. These adsorbent forces are responsible for attracting dyes to their surface. Some studies have shown that dye adsorption in MOFs is controlled by electrostatic interactions[31]. Therefore, the pH of the solution is expected to affect the amount of dye adsorbed as a result of the presence or absence of electrical charges on the dye molecules and the adsorbent surface. These dyes have a positive charge at the mentioned optimal pH and according to the results of the zeta potential analysis and the negativity of the surface charge of the absorbent, the adsorption process occurs due to the electrostatic interaction between the cationic dye and the absorbent surface.

### Sorbent efficiency in removing other dyes

Industrial effluents and aqueous solutions are a mixture of various pollutants, including organic dyes. The selectivity of a sorbent is important if it can separate a group of specific dyes from other pollutants, and it is one of the features that are considered in the manufacture of sorbents. In this study, magnetic composite MgFe$_2$O$_4$-NH$_2$-HKUST-1 can absorb cationic dyes such as malachite green, crystal violet, and methylene blue while two anionic dyes, metal orange, and methyl red, are not adsorbed on the sorbent surface. This feature can be an advantage for the studied absorber. Figure 6 shows the high adsorption capacity of the sorbent used for cationic dyes, while the adsorption capacity for the other two anionic pollutants is very small.

Comparison with other studies

The synthesized magnetic adsorbent was compared with some adsorbents to remove of MG, CV, and MB and shown in Table 6. As it is known, the synthesized adsorbent shows a good absorption capacity and extremely short time of 5 min for the absorption process. Also, the ability to easily separate the adsorbent with an external magnet is a special feature of the synthesized adsorbent compared to non-magnetic adsorbents.

Conclusion

In this research, magnetic adsorbent MgFe$_2$O$_4$-NH$_2$-HKUST-1 was synthesized as an efficient adsorbent in absorbing malachite green, crystal violet, and methylene blue. The results showed that the synthesized adsorbent has a negative surface charge that creates an electrostatic attraction between the cationic dyes and the adsorbent surface. The results of this study showed that the adsorption capacity of the magnetic adsorbent is equal to 108.69 mg g^{-1} for MG, 70.42 mg g^{-1} for CV, and 156.25 mg g^{-1} for MB. It was observed that malachite green, crystal violet, and methylene blue respectively at pH = 5.5, 5, and 7 at the optimum time of 5 min, and amounts of adsorbent 10, 5.5, and 1 mg were removed more than 75%. The synthesized adsorbent has a high potential to remove dyes in a very short contact time. In addition, this absorbent with its magnetic property is very quickly and easily collected by an external magnet from the working environment, which easily eliminates the difficult and time-consuming step of separating the solid phase from the solution and using a centrifuge. So the process
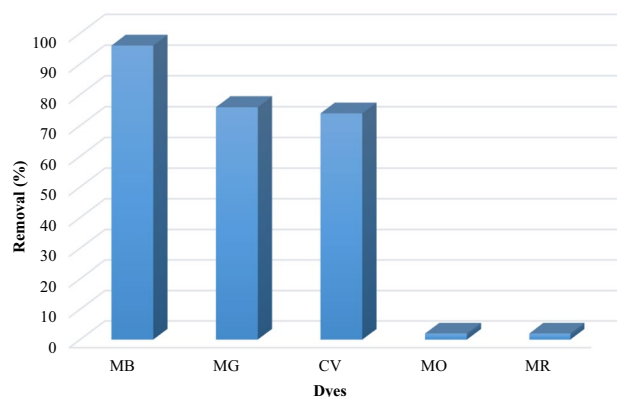
Figure 6. Comparison of the performance of the synthetic composite for removing different dyes.

Dye	Adsorbent	Time (min)	$q_{max\ (mg/g)}$	References
MG	MIL-53(Al)	30	81.2	[32]
	Fe-BTC	30	177	[33]
	MgFe$_2$O$_4$-NH$_2$-HKUST-1	5	108.69	Present study
CV	SH NH$_2$-MIL-125 (Ti)	180	129.87	[34]
	H$_2$dtoaCu	100	165.83	[35]
	MgFe$_2$O$_4$-NH$_2$-HKUST-1	5	70.42	Present study
MB	HKUST-1	40	101	[36]
	Amin-MOF-Fe	180	312.5	[37]
	MgFe$_2$O$_4$-NH$_2$-HKUST-1	5	156	Present study

Table 6. Comparison of adsorption capacities of MG, CV, and MB using various MOFs obtained in the present work and reported in the literature.

of absorbing by this absorbent is an efficient, fast, and economical process. MgFe$_2$O$_4$-NH$_2$-HKUST-1 composite as a magnetic adsorbent can be a promising future for environment-based processes.

Data availability

All data generated or analyzed during this study are included in this published article.

References

1. Gao, Q., Xu, J. & Bu, X. H. Recent advances about metal–organic frameworks in the removal of pollutants from wastewater. *Coord. Chem. Rev.* **378**, 17–31 (2019).
2. Lee, S. *et al.* Fast and sensitive trace analysis of malachite green using a surface-enhanced Raman microfluidic sensor. *Anal. Chim. Acta* **590**, 139–144 (2007).
3. Mani, S. & Bharagava, R. N. Exposure to crystal violet, its toxic, genotoxic and carcinogenic effects on environment and its degradation and detoxification for environmental safety. *Rev. Environ. Contam. Toxicol.* **237**, 71–104 (2016).
4. Mohammadnejad, M., Hajiashrafi, T. & Rashnavadi, R. Highly efficient determination of malachite green in aquatic product using Tb-organic framework as sorbent. *J. Porous Mater.* **25**(6), 1771–1781 (2018).
5. Srivastava, S., Sinha, R. & Roy, D. Toxicological effects of malachite green. *Aquat. Toxicol.* **66**(3), 319–329 (2004).
6. Cha, C. J., Doerge, D. R. & Cerniglia, C. E. Biotransformation of malachite green by the fungus *Cunninghamella elegans*. *Appl. Environ. Microbiol.* **67**(9), 4358–4360 (2001).
7. Tan, I. A. W., Ahmad, A. L. & Hameed, B. H. Adsorption of basic dye on high-surface-area activated carbon prepared from coconut husk: Equilibrium, kinetic and thermodynamic studies. *J. Hazard. Mater.* **154**(1–3), 337–346 (2008).
8. Tan, I. A. W., Ahmad, A. L. & Hameed, B. H. Adsorption of basic dye using activated carbon prepared from oil palm shell: Batch and fixed bed studies. *Desalination* **225**(1–3), 13–28 (2008).
9. Haik, Y., Qadri, S., Ganoe, A., Ashraf, S. & Sawafta, R. Phase change material for efficient removal of crystal violet dye. *J. Hazard. Mater.* **176**(1–3), 1110–1112 (2010).
10. James, S. L. Metal-organic frameworks. *Chem. Soc. Rev.* **32**(5), 276–288 (2003).
11. Zhou, H.-C. Introduction to metal–organic frameworks. *Chem. Rev.* **112**, 673–674 (2012).
12. Jiao, L., Wang, Y., Jiang, H. L. & Xu, Q. Metal–organic frameworks as platforms for catalytic applications. *Adv. Mater.* **30**(37), 1–23 (2018).
13. Ghanbari, T., Abnisa, F. & Daud, W. M. A. W. A review on production of metal organic frameworks (MOF) for CO$_2$ adsorption. *Sci. Total Environ.* **707**, 135090 (2020).

14. Naseri, M. *et al.* Lipase and laccase encapsulated on zeolite imidazolate framework: Enzyme activity and stability from voltammetric measurements. *ChemCatChem* **10**(23), 5425–5433 (2018).
15. Lustig, W. P. *et al.* Metal-organic frameworks: Functional luminescent and photonic materials for sensing applications. *Chem. Soc. Rev.* **46**(11), 3242–3285 (2017).
16. Au, V. K. M. Recent advances in the use of metal-organic frameworks for dye adsorption. *Front. Chem.* **8**(August), 1–7 (2020).
17. Chui, S.S.-Y., Lo, S.M.-F., Charmant, J. P. H., Orpen, A. G. & Williams, I. D. A chemically functionalizable nanoporous material [Cu$_3$(TMA)$_2$(H$_2$O)$_3$]$_n$. *Science* **283**(5405), 1148–1150 (1999).
18. Mohammadian, R., Karimi Alavijeh, M., Kamyar, N., Amini, M. M. & Shaabani, A. Metal–organic frameworks as a new platform for molecular oxygen and aerobic oxidation of organic substrates: Recent advances. *Polyhedron* **156**, 174–187 (2018).
19. Dhaka, S. *et al.* Metal–organic frameworks (MOFs) for the removal of emerging contaminants from aquatic environments. *Coord. Chem. Rev.* **380**, 330–352 (2019).
20. Demarchi, C. A., Campos, M. & Rodrigues, C. A. Adsorption of textile dye Reactive Red 120 by the chitosan-Fe(III)- crosslinked: Batch and fixed-bed studies. *J. Environ. Chem. Eng.* **1**(4), 1350–1358 (2013).
21. Ahmed, I. & Jhung, S. H. Composites of metal-organic frameworks: Preparation and application in adsorption. *Mater. Today* **17**(3), 136–146 (2014).
22. Aoopngan, C. *et al.* Amine-functionalized and hydroxyl-functionalized magnesium ferrite nanoparticles for Congo red adsorption. *ACS Appl. Nano Mater.* **2**(8), 5329–5341 (2019).
23. Wu, G. *et al.* Magnetic copper-based metal organic framework as an effective and recyclable adsorbent for removal of two fluoroquinolone antibiotics from aqueous solutions. *J. Colloid Interface Sci.* **528**, 360–371 (2018).
24. Zhang, Q. *et al.* A porous metal-organic framework with –COOH groups for highly efficient pollutant removal. *Chem. Commun.* **50**(92), 14455–14458 (2014).
25. Tian, H., Peng, J., Lv, T., Sun, C. & He, H. Preparation and performance study of MgFe$_2$O$_4$/metal–organic framework composite for rapid removal of organic dyes from water. *J. Solid State Chem.* **257**, 40–48 (2018).
26. Hu, S. *et al.* Facile synthesis of Fe$_3$O$_4$/g-C$_3$N$_4$/HKUST-1 composites as a novel biosensor platform for ochratoxin A. *Biosens. Bioelectron.* **92**, 718–723 (2017).
27. Zhao, X. *et al.* Synthesis of magnetic metal-organic framework (MOF) for efficient removal of organic dyes from water. *Sci. Rep.* **5**(July), 1–10 (2015).
28. Xie, W. & Wan, F. Basic ionic liquid functionalized magnetically responsive Fe$_3$O$_4$@HKUST-1 composites used for biodiesel production. *Fuel* **220**, 248–256 (2018).
29. Sharma, A. *et al.* Cobalt ferrite incorporated *Ocimum sanctum* nanocomposite matrix as an interface for adsorption of organic dyes: A sustainable alternative. *ChemistrySelect* **8**(5), e202203709 (2023).
30. Sharma, A., Mangla, D., Choudhry, A., Sajid, M. & Chaudhry, S. A. Facile synthesis, physico-chemical studies of *Ocimum sanctum* magnetic nanocomposite and its adsorptive application against Methylene blue. *J. Mol. Liq.* **362**, 119752 (2022).
31. Hasanzadeh, M., Simchi, A. & ShahriyariFar, H. Nanoporous composites of activated carbon-metal organic frameworks for organic dye adsorption: Synthesis, adsorption mechanism and kinetics studies. *J. Ind. Eng. Chem.* **81**, 405–414 (2020).
32. Al Sharabati, M. & Sabouni, R. Selective removal of dual dyes from aqueous solutions using a metal organic framework (MIL-53(Al)). *Polyhedron* **190**, 114762 (2020).
33. Delpiano, G. R., Tocco, D., Medda, L., Magner, E. & Salis, A. Adsorption of malachite green and alizarin red s dyes using Fe-BTC metal organic framework as adsorbent. *Int. J. Mol. Sci.* **22**(2), 1–16 (2021).
34. Wen, G. & Guo, Z. Facile modification of NH2-MIL-125 (Ti) to enhance water stability for efficient adsorptive removal of crystal violet from aqueous solution. *Colloids Surf. A Physicochem. Eng. Asp.* **541**, 58–67 (2018).
35. Li, X. *et al.* Adsorption removal of crystal violet from aqueous solution using a metal-organic frameworks material, copper coordination polymer with dithiooxamide. *J. Appl. Polym. Sci.* **129**(5), 2857–2864 (2013).
36. Kaur, R., Kaur, A., Umar, A., Anderson, W. A. & Kansal, S. K. Metal organic framework (MOF) porous octahedral nanocrystals of Cu-BTC: Synthesis, properties and enhanced absorption properties. *Mater. Res. Bull.* **109**, 124–133 (2019).
37. Paiman, S. H. *et al.* Functionalization effect of Fe-type MOF for methylene blue adsorption. *J. Saudi Chem. Soc.* **24**(11), 896–905 (2020).

Acknowledgements

Author contributions
N.M.N., S.A. and S.S. synthesized the component and did all experimental analysis. M.M., N.M.N. and S.A. wrote the main manuscript text and S.G. edited characterization section. M.M. and S.G. reviewed the manuscript.

Competing interests
The authors declare no competing interests.

Additional information
Correspondence and requests for materials should be addressed to M.M.

Reprints and permissions information is available at www.nature.com/reprints.

Publisher's note Springer Nature remains neutral with regard to jurisdictional claims in published maps and institutional affiliations.